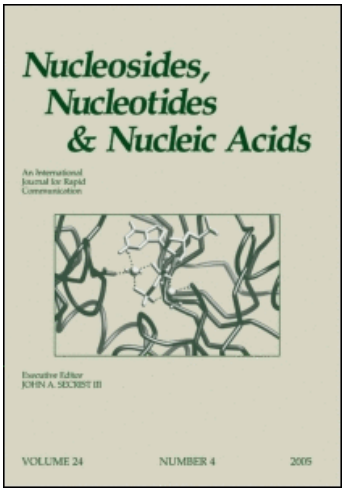

Nucleosides, Nucleotides and Nucleic Acids
Publication details, including instructions for authors and subscription information:
http://www.informaworld.com/smpp/title~content=t713597286

Fluorescent α-Anomeric 1,N(6)Etheno- Deoxyadenosine in DNA Duplexes. the α-εdA / dG Pair

L. Bielecki[a]; B. Skalski[b]; I. Zagórowska[a]; R. E. Verrall[c]; R. W. Adamiak
[a] Institute ofBioorganic Chemistry, Polish Academy of Sciences, Poznañ, Poland [b] Faculty of Chemistry, Adam Mickiewicz University, Poznañ, Poland [c] Department of Chemistry, University of Saskatchewan, Saskatoon, Saskatchewan, Canada

To cite this Article Bielecki, L. , Skalski, B. , Zagórowska, I. , Verrall, R. E. and Adamiak, R. W.(2000) 'Fluorescent α-Anomeric 1,N(6)Etheno- Deoxyadenosine in DNA Duplexes. the α-εdA / dG Pair', Nucleosides, Nucleotides and Nucleic Acids, 19: 10, 1735 — 1750
To link to this Article: DOI: 10.1080/15257770008045456
URL: http://dx.doi.org/10.1080/15257770008045456

NUCLEOSIDES, NUCLEOTIDES & NUCLEIC ACIDS, 19(10–12), 1735–1750 (2000)

FLUORESCENT α-ANOMERIC 1,N(6)ETHENO- DEOXYADENOSINE IN DNA DUPLEXES. THE α-εdA / dG PAIR ⊗

L. Bielecki, B. Skalski[1], I. Zagórowska, R. E. Verrall[2] and R. W. Adamiak*

Institute of Bioorganic Chemistry, Polish Academy of Sciences, Poznań, Poland,
[1]Faculty of Chemistry, Adam Mickiewicz University, Poznań, Poland
[2]Department of Chemistry, University of Saskatchewan, 110 Science Place, Saskatoon, Saskatchewan S7N 5C9, Canada.

ABSTRACT: Structural properties of the fluorescent α-anomeric 1,N(6)etheno-deoxyadenosine residue placed in opposition to all four canonical deoxynucleotide units within 11-mer DNA duplexes have been studied. The duplex with α-εdA / dG pairing is most thermodynamically stable while the α-εdA / dC one is the least stable. Fluorescence measurements confirm the thermodynamic data and indicate base-pair dependent stacking properties of α-εdA within duplex structures. Results of molecular dynamics (MD) simulations in aqueous solution for the most stable duplex point to the presence of different conformational states of the α-1,N(6)etheno-deoxyadenosine residue, including formation of a hydrogen bonded pair with the dG and possible occurrence of severe kinking in the duplex.

The structures of short DNA duplexes containing fluorescent 1,N(6)etheno-deoxyadenosine have been reported using NMR[1] and X-ray crystallography methods[2]. In both cases the formation of two non-classical hydrogen bonds between the deoxyguanosine residue and *syn* 1,N(6)etheno-deoxyadenosine units was observed; the modified base being well accommodated within the interior of rather uniform DNA duplexes. Results of our ongoing fluorescence studies on DNA duplexes containing 1,N(6)etheno-deoxyadenosine suggested that the β to α reversal of configuration at the C1' anomeric site might orient the modified fluorescent base towards the exterior of the duplex making the fluorophore more accessible to environmental factors of interest.

⊗ article *in memoriam* of the late Professor Alexander Krayevski

*corresponding author; tel.:+48-61 8528503, fax.:+48-61 8520503, e-mail: adamiakr@ibch.poznan.pl

Knowledge of the geometry of the α-anomeric fluorophore within a DNA duplex will provide useful comparative information in the future evaluation of the behaviour of α-anomeric green-yellow fluorophores of the luminarosine group[3-5] in such systems. Also, it will be of relevance in determining the influence of unmodified α-nucleotide residues on the DNA structure[6].

In order to test our hypothesis a set of four 11-mer DNA duplexes was prepared in which a single α-1,N(6)etheno-deoxyadenosine residue was placed in opposition to all four canonical nucleobases. The results of thermodynamic and time-resolved fluorescence studies presented herein reveal that all the modified duplexes form stable structures in a similar manner to the four unmodified reference duplexes. The duplex with the α-εdA / dG base opposition is most stable. This result prompted us to evaluate the possible influence of the α-anomeric 1,N(6)etheno-deoxyadenosine residue on the global structure of a short DNA duplex using the molecular dynamics simulation approach. The results of the MD simulation in aqueous solution for the α-εdA / dG duplex reveal that the tricyclic base has a tendency to be buried into the helix interior. This leads to the formation of a non-classical base pair with the dG residue and the inducement of severe kinking of the DNA duplex.

RESULTS AND DISCUSSION

Chemistry

α-Deoxyadenosine prepared *via* trans-ribosylation[7] was transformed into α-1,N(6)etheno-deoxyadenosine using a procedure originally developed for the ribo-series[8] but under elevated pH since this deoxynucleoside is prone to depurination. All other protected deoxynucleosides, their 3'-(2-cyanoethyl)(N,N-diisopropyl)-phosphoramidites and oligodeoxynucleotides d($^{5'}$CTCCTα-εATCCCT$^{3'}$), d($^{5'}$CTCCTXTCCCT$^{3'}$) [X=T,C,A,G] and d($^{5'}$AGGGAXAGGAG$^{3'}$) [X=T,C,A,G] were synthesised according to the standard protocols.

Thermodynamics of α-εdA - modified DNA duplexes using an UV melting method

Oligodeoxynucleotides were annealed in a 1:1 ratio at pH=7.0 to form 11 bp duplexes of the following general sequence:

d ($^{5'}$CTCCTXTCCCT$^{3'}$)	where X stands for α-εA or dC (as reference)
d ($^{3'}$GAGGAYAGGGA$^{5'}$)	where Y stands for T, dC, dA and dG

For reference purposes with the four modified duplexes, four unmodified duplexes were prepared in which deoxycytidine units were substituted for α-1,N(6)etheno-deoxyadenosine.

Both sets of duplexes were subjected to thermodynamical analysis using UV melting data. Two methods were applied: (i) values of ΔH° and ΔS° were estimated from a plot of reciprocal melting temperature (T_M^{-1}) versus the logarithm of (C_T/4) based on

TABLE 1. Thermodynamic parameters of the reference DNA duplex formation in 1M NaCl

DNA *vs*	T_M^{-1} *vs* log (C_T/4)				av from fits			
	$-\Delta H^\circ$ (kcal/mol)	$-\Delta S^\circ$ (eu)	$-\Delta G^\circ_{37^\circ C}$ (kcal/mol)	T_M (°C) at 10^{-4}M	$-\Delta H^\circ$ (kcal/mol)	$-\Delta S^\circ$ (eu)	$-\Delta G^\circ_{37^\circ C}$ (kcal/mol)	T_M (°C) at 10^{-4}M
C / T	85.1	249.8	7.6	41.1	82.7	242.2	7.6	41.2
C / C	60.2	173.1	6.5	36.8	71.0	208.4	6.4	36.3
C / A	60.7	171.8	7.5	41.8	76.4	221.2	7.5	41.0
C / G	108.9	310.7	12.6	55.3	94.5	266.2	12.0	55.7

TABLE 2. Thermodynamic parameters of the modified DNA duplex formation in 1M NaCl

DNA *vs*	T_M^{-1} *vs* log (C_T/4)				av from fits			
	$-\Delta H^\circ$ (kcal/mol)	$-\Delta S^\circ$ (eu)	$-\Delta G^\circ_{37^\circ C}$ (kcal/mol)	T_M (°C) at 10^{-4}M	$-\Delta H^\circ$ (kcal/mol)	$-\Delta S^\circ$ (eu)	$-\Delta G^\circ_{37^\circ C}$ (kcal/mol)	T_M (°C) at 10^{-4}M
αεA / T	93.3	275.9	7.7	41.1	82.4	240.7	7.7	41.5
αεA / C	95.0	284.3	6.9	38.2	72.2	210.4	7.0	38.9
αεA / A	55.8	156.3	7.3	41.5	68.8	197.8	7.4	41.0
αεA / G	70.5	200.1	8.10	44.0	91.2	265.9	8.7	44.6

equation: $T_M^{-1} = R/\Delta H^\circ \ln(C_T/4)+\Delta S^\circ/\Delta H^\circ$ as previously described[9,10] and (ii) averaging of ΔH° and ΔS° values from fits of individual melting curves[11]. The uniform melting curves and evaluated T_M values clearly show that duplex structures formed are very stable in reference to DNA containing the CG base pair and CT, CC and CA mismatches (Table 1 and 2). However, results obtained for modified DNA duplexes indicate that the ΔH° values determined from (T_M^{-1}) versus ln (C_T/4) plots and from curve fitting differ by more than 13% i.e. a typical error estimate for ΔH°. This could indicate the presence of molecules having anomalous two-state transitions.

The α-εdA modification can be considered to be similar to the formation of a single internal loop (mismatch) and the free energy of loop formation[12] was estimated from the relation: $\Delta G^\circ_{37^\circ C(loop)} = \Delta G^\circ_{37^\circ C(modified\ duplex)} - \Delta G^\circ_{37^\circ C(duplex)} + \Delta G^\circ_{37^\circ C(NN)}$

where $\Delta G^\circ_{37^\circ C(modified\ duplex)}$ is the free energy of formation of the duplex containing a modified pair treated as mismatch, $\Delta G^\circ_{37^\circ C(duplex)}$ is the free energy of an unmodified duplex of sequence $^{5'}$CTCCTTCCCT$^{3'}$ $^{3'}$GAGGAAGGGA$^{5'}$ (-11.6 kcal/mol; based on the nearest neighbour principle[13]) and $\Delta G^\circ_{37^\circ C(NN)}$ is the free energy for the nearest neighbour $^{5'}$TT$^{3'}$+$^{5'}$AA$^{3'}$ = -1,7 kcal/mol which was interrupted by an internal loop. The estimated $\Delta G^\circ_{37^\circ C(loop)}$ values [kcal/mol] for α-εdA *vs* T, dC, dA and dG are 2.2, 3.0, 2.6 and 1.8, respectively, i.e. above the range observed for canonical base DNA mismatches[14] . It is clear that α-εdA / dG is the most stable opposing base pair within the studied set.

TABLE 3. Fluorescence quantum yields and decay parameters from three exponential fits.

DNA	λ_{max} [nm]	$\phi/\phi_{\varepsilon A}$	τ_1 (A_1) [ns]	τ_2 (A_2) [ns]	τ_3 (A_3) [ns]	χ^2	$\langle\tau\rangle^*$ [ns]	$\langle\tau\rangle/\tau_{\varepsilon A}$
εA	412	1	26.8			1.05		
S	407	0.06	6.35 (0.57)	2.24 (0.34)	0.72 (0.09)	1.09	5.57	0.21
T	408	0.14	16.41 (0.58)	5.26 (0.37)	1.49 (0.05)	1.14	14.41	0.54
C	405	0.13	9.60 (0.62)	3.50 (0.34)	0.97 (0.04)	0.90	8.53	0.32
A	408	0.17	12.37 (0.58)	5.60 (0.37)	1.30 (0.05)	1.06	10.78	0.40
G	408	0.19	10.02 (0.87)	5.78 (0.12)	0.48 (0.01)	0.96	9.69	0.36

S- stands for single stranded d(CTCCTα-εATCCCT). Intensity average lifetime $\langle\tau\rangle = \Sigma A_i\tau_i^2 / \Sigma A_i\tau_i$

Results of steady state and time resolved fluorescence measurements

As revealed by steady state fluorescence measurements, the quantum efficiency of α-εdA incorporated into a single stranded d(CTCCTα-εATCCCT) decreases to ca. 1/17 that of free α-εdA, with a concomitant, slight blue shift of the fluorescence maximum (Table 3). Upon duplex formation, the fluorescence intensity of the α-1,N(6)-ethenoadenosine labelled single stranded oligodeoxynucleotide increases with little, if any, change in the position of the fluorescence maximum (Fig. 1A). Fig. 1B shows the plots of integral fluorescence intensities *vs* the molar equivalent of added non-fluorescent complementary strand in the formation of all four duplexes at neutral pH.

As can be seen, in each case, increasing concentration of the complementary strand results in a gradual increase in fluorescence intensity at 410 nm until a plateau is reached indicating completion of the hybridisation process. The largest increase (ca. 3.2 fold) in the fluorescence intensity occurs for the α-εdA / dG duplex formation and its magnitude decreases in the following order: dG > dA> T ≥ dC. Furthermore, it should be noted in the case of α-εdA / dG duplex formation, that complete hybridisation is achieved at a concentration of the complementary strand, dG, corresponding to ca. 1.3 molar equivalent of the fluorescent strand. On the other hand, formation of the other three duplexes requires almost two-fold excess of the respective non-fluorescent strands. In each case the final fluorescence intensity of duplexes formed did not change after heating the solutions up to 80°C followed by slow cooling to initial temperature (15°C) at which titrations were performed.

Fluorescence melting profiles for all duplexes are shown in Fig. 2 as Stern-Volmer fluorescence quenching plots. The plots for α-εdA / dG, T and dA duplexes exhibit characteristic sigmoidal shape for the melting process, whereas that for the α-εdA / dC duplex shows almost linear dependence over the entire temperature range. The estimated melting temperatures are a bit lower than those obtained from the UV-melting profiles, however, they decrease in a similar order:

α-εdA / dG (42°C) > α-εdA / T (35°C) ≅ α-εdA / dA (33°C).

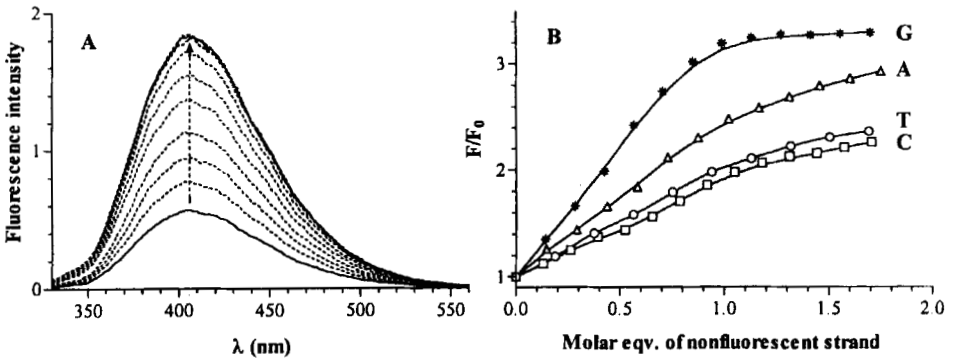

FIG. 1. (A) Changes in the fluorescence spectrum of the α-εdA labeled single stranded oligonucleotide (solid line) upon addition of nonfluorescent strand dG. (B) The plots of corresponding integral fluorescence intensities *vs* molar equivalent of the nonfluorescent strand for the formation of all four duplexes.

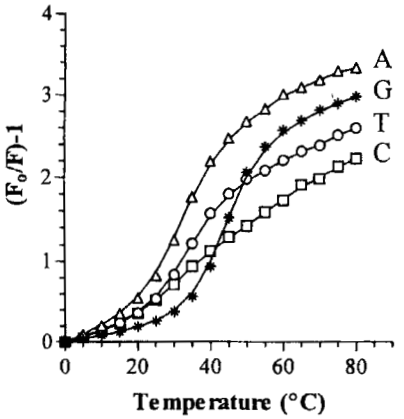

FIG. 2. Fluorescence melting profiles for α-εdA labelled duplexes

The lower T_M values obtained from fluorescence measurements, compared with UV profiles, may result from the fact that the latter were obtained at higher concentrations of duplexes. On the other hand, one must remember that fluorescence is very sensitive to small changes in fluorophore micro-environment and therefore, lower T_M values may also reflect "local" structural changes occurring within the duplexes before complete dissociation.

The fluorescence maxima and relative quantum yields of the four duplexes α-εdA / T, dC, dA and dG, measured *vs* free α-εdA, are summarised in Table 3 together with the corresponding fluorescence lifetime data obtained from fitting of the decay curves measured at 2°C, i.e. well below the melting temperatures. As can be seen, the position of emission of α-εdA changes little upon hybridisation. Even though the fluorescence efficiency increases upon hybridisation, the quenching in duplexes is still efficient and in the case of the α-εdA / dG duplex, for which the highest fluorescence enhancement is observed, the quantum yield reaches only ca. 19% that of free α-εdA. The fluorescence spectra of both single stranded oligodeoxynucleotide and all four duplexes decays nonexponentially and a sum of three exponential decays is required to fit the decay curves reasonably well. The component lifetimes and corresponding amplitudes can be used to calculate the intensity average lifetimes for each of the decays (Table 3).

As would be expected, the most pronounced fluorescence lifetime shortening occurs in the case of d(CTCCTα-εATCCCT) for which the intensity average lifetime decreases to ca. 1/5 of that of free α-εdA. However, as one can see, there is no simple correlation between the fluorescence quantum yields and the average lifetimes in the case of the duplexes.

Comparison of the data in Table 3 reveals that in each case the decrease in the lifetimes of the oligonucleotides is considerably less than that of the respective fluorescence quantum yields. This indicates that a static quenching process dominates the overall fluorescence quenching of the oligonucleotides, and furthermore, that the relative contributions of dynamic and static processes vary substantially among those structures. In each of the four duplexes the α-εdA residue is flanked by two thymidines and each duplex differs only in the central base of the complementary strand (opposite to the α-εdA fluorophore). Therefore the observed differences in fluorescence quantum yields and lifetimes must reflect structural differences resulting mainly from a different degree of base stacking and different "base-pairing" type interactions of α-εdA within the duplex structures.

Efficient and sequence dependent quenching of α-εdA was previously observed for di-ribonucleoside monophosphates combining 1,N(6)etheno-adenosine with all canonical ribonucleosides[15] as well as for chloroacetaldehyde-modified poly(A) and similar structures[16,17]. It is generally accepted that fluorescence emission is quenched in both dynamic and static processes by all of the neighbouring nucleosides involved in stacking interactions with the fluorophore.

Fig. 3 shows the fluorescence excitation spectra of the single strand and duplexes α-εdA / dG and α-εdA / dC, scanned over the long wavelength absorption band of 1,N(6)etheno-adenine. The spectra are normalised at 310 nm and compared with those of the unbound α-εdA. As one can see, the long wavelength excitation band of α-εdA in oligonucleotidic structures undergoes a clear bathochromic shift. This shift is particularly large in the case of the α-εdA / dC duplex indicating, most likely, that the highest degree of base stacking interaction of the 1,N(6)etheno-adenine with neighbouring bases occurs in this structure.

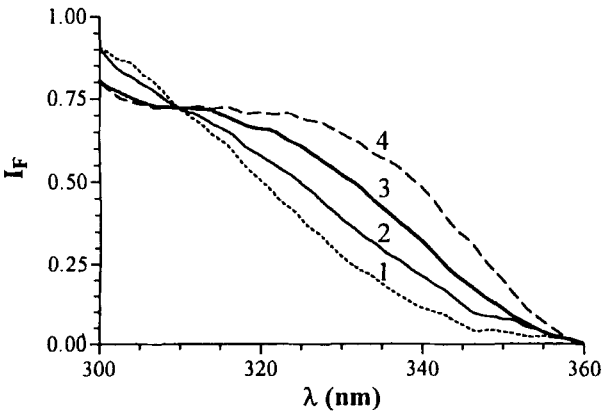

FIG. 3. Comparison of the long wavelength bands of the fluorescence excitation spectra of the α-εdA / C (4) and α-εdA / G (3) duplexes with those for single stranded oligonucleotide d(CTCCTα–εATCCCT) (2) and free α-1,N(6)-ethenoadeoxyadenosine (1). The spectra are normalised at 310 nm.

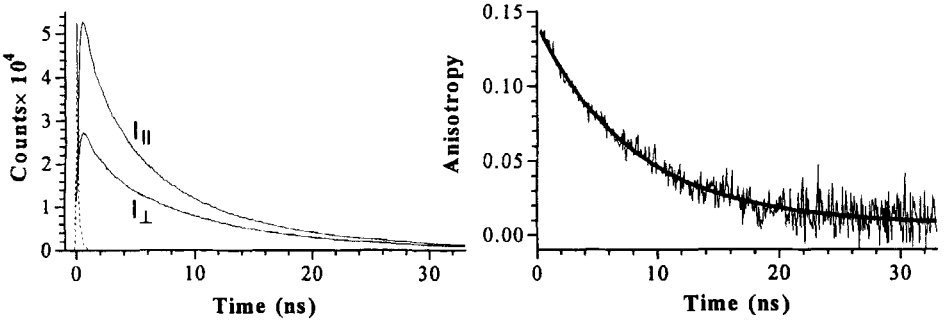

FIG. 4. Time-dependent polarised decays for the α-εdA / dG duplex at 2 °C (left) and the calculated anisotropy decay (right). The corresponding fitting parameters are listed in Table IV together with the respective data for the other three duplexes.

Fig. 4 shows the fluorescence anisotropic decay of the α-εdA / dG duplex, extracted from parallel ($I_{\|}$) and perpendicular ($I_{\perp}$) decay curves using the equation[18]:

$r(t) = (I_{\|} - I_{\perp}) / (I_{\|} + 2I_{\perp})$

The curve was fitted by a single exponential decay function: $r(t) = r_o \exp(-t/\tau_r)$

where r_o is the anisotropy at zero time and τ_r is rotational correlation time.

In the case of the single stranded oligonucleotide and the remaining three duplexes, a sum of two exponentials was required to obtain satisfactory fits of the anisotropic decays. The best fit parameters, r_{oi} and τ_{ri}, for all oligonucleotides are summarised in Table 4. The observed maximum values of zero time anisotropy are between 0.12 and 0.15 and correlate well with those obtained from the steady state excitation anisotropy spectra of the 1,N(6)etheno-adenosine fluorophore, measured at low temperatures[19,20]. The longer rotational correlation times obtained from fitting anisotropic decays reflect, most likely, the overall rotation of the oligonucleotidic structures. In the case of the α-εdA / dG and α-εdA / dA duplexes, the rotational correlation times fall in the range typical of regular DNA oligomers of the same size[21] whereas those for duplexes α-εdA / dT and, in particular, α-εdA / dC are significantly longer.

DNA	r_{oi}	τ_{ri} [ns]	χ^2
α-εA / G	0.135	8.13	1.15
α-εA / A	0.094	8.00	1.08
	0.052	2.87	
α-εA / C	0.076	12.35	1.11
	0.065	1.27	
α-εA / T	0.060	9.62	1.05
	0.062	1.13	
S	0.077	3.70	1.14
	0.061	0.74	

TABLE 4. Rotational correlation times and anisotropy amplitudes from fitting the experimental anisotropy decay curves measured at +2 °C.
S - stands for single stranded d(CTCCTα-εATCCCT).

Assuming that a straight duplex would rotate more rapidly around the long axis than a bent one, the unusually long rotational time of the α-εdA / dC could be rationalised in terms of the inducement of severe kinking by α-εdA in this particular structure.

As can be seen, there is also significant variation in the short rotational correlation times. It is quite reasonable to assume that these differences reflect different rotational freedom of the ethenoadenine residue within oligonucleotide structures. Thus, in the case of the structures with more internal rotational freedom of bases, one should expect these rotations to be faster. In agreement with this assumption the shortest correlation time of the fast rotating component is observed in the case of the single stranded fragment. On the other hand, in the case of the most stable duplex α-εdA / dG, in which the rotational freedom of α-εdA is strongly blocked, the fast anisotropy component is not observed.

Simulation of molecular dynamics of the α-εdA / dG DNA duplex

The spectrofluorimetry results obtained encouraged us to look at the structural image of these systems using advanced molecular dynamics simulation methods based on the Amber force field[22]. Simulations in aqueous solution of 1 ns duration were carried out (see Experimental for details) using the particle-mesh Ewald summation method[23] for treatment of long-range electrostatic forces. This latter approach has become widely used and commonly accepted in recent years[24] and is considered as the method providing the best representation of nucleic acids in aqueous medium. As the model molecule, it was decided to select the most stable α-εdA / dG duplex. The duplex containing the canonical C / G base pair was also simulated for reference. Two simulation runs were carried out for the modified system (one of them was subsequently extended to 1.1 ns), and one for the reference molecule. The results were quite surprising. Table 5 presents the mean values and standard deviations for selected helical parameters calculated using the CURVES 5.1 program[25] for selected periods of the three trajectories obtained. Since the anomerisation severely distorts the local coordinates system implemented in the CURVES 5.1, it was necessary to redefine it by changing the names of the C(4) and C(8) atoms of the modified residue and ignoring that residue in global axis calculation.

The most noteworthy structural features of the modified duplex are as follows. For the α-εdA residue, uncommon values of the sugar pseudorotational angle stabilised within the West conformation range were observed around 210° (trajectory #1) and around 310° (trajectory #2). Other nucleotide residues in all simulations usually maintained sugar conformations close to those typical for B-DNA. It must be noted (Table 5) that helical parameters calculated for the two base-paired segments adjacent to the modification site compare well with the reference molecule (C / G).

In simulation #1, a distinct kink could be identified in the middle region of the modified duplex, which can be attributed to the α-anomerisation while, surprisingly, in simulation #2 the duplex remained rather straight (cf. Fig. 5). No kinking[26] was observed in the case of the unmodified reference duplex.

TABLE 5. Mean values and standard deviations (in brackets) for selected helical parameters calculated using the CURVES 5.1 program[25] for the final periods of the two α-εdA / dG trajectories [α-εA (1) and α-εA(2)] and reference duplex (dC / dG) trajectory (C). For α-εA(1) and C, final 250 ps of simulation were taken for evaluation. αεA (2a) is the 750-950 ps range (before the conformational change) and α-εA(2b) is the extended 1.0-1.1 ns range.

base pair parameters												
param.	x-displacement [Å]				inclination [deg]				propeller twist [deg]			
X	αεA (1)	αεA (2a)	αεA (2b)	C	αεA (1)	αεA (2a)	αεA (2b)	C	αεA (1)	αεA (2a)	αεA (2b)	C
C1-G11	-1.6(0.7)	-2.3(0.8)	-1.7(0.7)	-1.6(0.8)	-10(7)	-5(6)	-7(6)	-10(7)	-3(13)	-8(15)	1(13)	11(13)
T2-A10	-1.6(0.8)	-2.1(0.7)	-1.7(0.7)	-1.7(0.8)	-13(7)	-9(6)	-8(7)	-13(7)	-6(10)	-10(11)	-6(12)	-7(12)
C3-G9	-1.7(0.7)	-2.1(0.7)	-1.8(0.6)	-1.8(0.7)	-13(6)	-10(6)	-7(5)	-14(7)	-7(12)	-10(10)	-6(10)	-5(10)
C4-G8	-1.5(0.8)	-2.0(0.6)	-1.8(0.6)	-1.8(0.7)	-16(6)	-12(5)	-10(5)	-16(6)	-6(10)	-11(10)	-7(9)	2(11)
T5-A7	-1.4(0.7)	-2.0(0.5)	-1.9(0.6)	-1.7(0.7)	-14(6)	-11(6)	-10(5)	-16(7)	4(10)	-13(10)	-17(10)	1(11)
X6-G6	-0.9(0.5)	-3.8(0.6)	-2.8(0.6)	-1.8(0.7)	3(6)	4(6)	-7(6)	-14(6)	-33(13)	35(12)	6(10)	-1(13)
T7-A5	-1.7(0.9)	-1.0(0.5)	-1.5(0.6)	-1.8(0.7)	-5(6)	1(7)	-6(6)	-13(6)	-8(12)	-4(11)	-15(9)	-4(11)
C8-G4	-1.5(1.0)	-0.9(0.4)	-1.8(0.5)	-1.9(0.7)	-6(6)	-4(7)	-8(6)	-11(7)	4(14)	-9(12)	-5(11)	-2(13)
C9-G3	-1.6(0.9)	-1.0(0.5)	-1.7(0.6)	-1.9(0.7)	-10(6)	-9(6)	-11(7)	-10(7)	0(11)	-5(12)	0(10)	-2(10)
C10-G2	-1.6(0.9)	-1.3(0.5)	-1.8(0.6)	-2.0(0.7)	-13(7)	-7(8)	-12(6)	-7(8)	0(11)	2(10)	-5(10)	-1(11)
T11-A1	-1.6(0.9)	-0.7(0.5)	-1.7(0.7)	-1.6(0.7)	-13(7)	-6(11)	-10(6)	-3(10)	-2(15)	-11(17)	-11(14)	-13(14)

base pair segments parameters												
param.	tilt [deg]				roll [deg]				twist [deg]			
X	αεA (1)	αεA (2a)	αεA (2b)	C	αεA (1)	αεA (2a)	αεA (2b)	C	αεA(1)	αεA(2a)	αεA(2b)	C
C1-G11	-0.2(5.0)	-0.6(5.8)	0.6(5.9)	-0.9(5.3)	2.9(8.2)	-0.7(7.5)	1.2(7.8)	9.3(7.6)	27(4)	29(4)	28(4)	26(4)
T2-A10	2.8(5.2)	2.8(4.9)	3.4(5.0)	-0.2(5.6)	4.2(7.8)	0.2(8.3)	4.2(7.3)	3.1(8.1)	30(5)	33(5)	32(5)	30(4)
C3-G9	-4.2(5.0)	-2.8(4.7)	-2.3(5.1)	-2.6(5.3)	2.5(8.4)	1.3(7.4)	7.1(6.2)	2.2(8.0)	33(4)	31(4)	28(3)	29(4)
C4-G8	0.2(5.3)	0.9(5.3)	1.4(5.5)	-0.5(5.2)	-0.4(6.4)	-0.0(6.7)	2.6(6.9)	-0.8(7.9)	20(3)	33(4)	30(3)	26(4)
T5-A7	-11.3(5.9)	7.4(6.4)	4.6(5.2)	1.5(5.4)	3.5(7.1)	-4.3(8.8)	-4.8(7.6)	-1.2(8.0)	-39(6)	-26(5)	11(4)	30(5)
X6-G6	5.5(6.0)	-5.1(6.4)	-2.8(5.0)	0.2(5.3)	7.7(6.7)	19.9(7.4)	9.3(7.2)	3.7(7.9)	98(5)	69(4)	47(4)	27(4)
T7-A5	0.6(6.0)	3.3(5.1)	-1.2(5.8)	1.8(5.2)	4.4(8.7)	5.2(8.2)	8.2(7.1)	5.0(8.8)	30(4)	31(5)	28(4)	28(4)
C8-G4	0.4(6.3)	-1.9(4.8)	-1.4(5.1)	-1.6(5.7)	8.5(8.4)	4.0(6.7)	3.7(7.1)	2.2(9.3)	27(4)	30(4)	30(4)	29(4)
C9-G3	-0.2(4.9)	2.3(4.9)	-0.9(5.1)	-1.1(5.7)	0.4(8.3)	5.3(8.1)	1.8(7.4)	-0.5(7.6)	29(4)	28(4)	30(4)	32(4)
C10-G2	-0.5(6.2)	6.9(8.3)	-0.2(5.9)	3.7(7.6)	-0.9(9.2)	11.2(12.3)	1.8(9.8)	5.9(10.2)	29(5)	33(5)	31(4)	32(5)

pseudorotational angle ϕ [deg]									
	strand 1					strand 2			
X	αεA (1)	αεA (2a)	αεA (2b)	C	X	αεA (1)	αεA (2a)	αεA (2b)	C
C1	105(43)	124(29)	125(31)	123 (29)	A1	118(36)	133(33)	125(54)	109 (47)
T2	103(35)	100(27)	98(29)	110 (28)	G2	111(33)	151(38)	130(25)	151 (23)
C3	131(28)	136(20)	135(25)	120 (24)	G3	118(32)	109(23)	111(24)	121 (24)
C4	115(24)	119(22)	110(23)	109 (24)	G4	126(31)	117(29)	132(22)	111 (25)
T5	144(9)	69(41)	115(24)	105 (31)	A5	151(15)	142(14)	115(22)	107 (29)
X6	213(19)	314(39)	316(14)	92 (42)	G6	75(23)	150(11)	146(10)	97 (37)
T7	126(49)	93(34)	93(30)	76 (39)	A7	144(12)	139(40)	130(34)	63 (41)
C8	134(21)	134(28)	108(28)	107 (45)	G8	102(33)	129(21)	112(22)	45 (31)
C9	106(45)	106(24)	125(27)	133 (27)	G9	129(23)	117(24)	106(34)	26 (22)
C10	116(37)	128(24)	132(21)	140 (21)	A10	107(31)	125(24)	122(44)	17 (14)
T11	128(24)	107(33)	130(24)	110 (31)	G11	108(33)	118(28)	134(22)	152 (26)

A detailed analysis of the alignment of residues in the modified region provides a possible explanation to both conformational states observed. In the kinked duplex, severe changes of the backbone angles (data not shown) and tilt angle are observed both for the modified pair and for the C8-C9 segment of the modified strand, where

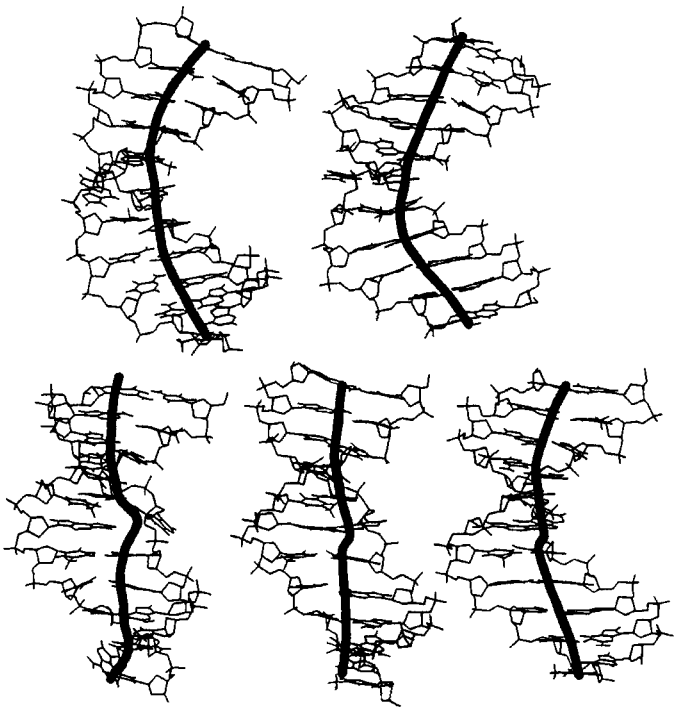

FIG. 5. Examples of the global structural images of the duplex modified with the α-εdA / dG pair. Top row - trajectory #1; stable kink. Bottom - trajectory #2; conformational transition in the middle of the duplex (from left to right). Major duplex axis calculated with CURVES 5.1[25]

a conformational compensation of the kink probably occurred. In trajectory #2, no major deviations from the unmodified duplex were observed. The structural image of the middle regions of the duplexes reveals further striking phenomena. In trajectory #1, the tricyclic εdA base is pushed to some extent towards the exterior of the duplex. It practically loses the stacking interactions to its neighbour bases but is still able to maintain a single hydrogen bond with the opposite guanine [N(2)-H···N(3); see Fig. 6]. On the other hand, the stacking interactions in the unmodified strand are very stable.

This tendency of the α-anomerised residue to protrude from the helix to the minor groove might account for the clearly observed kinking of the molecule (cf. Fig. 5).

Consequently, returning to our initial hypothesis, the nucleobase is directed to the outer sphere of the duplex but at the expense of DNA kink formation. For trajectory #2 of the modified molecule, a different situation is observed. The modified base maintains the stacking interactions with its neighbours, while the opposite base, guanine, is pushed towards the exterior and its stacking is much weakened. In the final period of the simulation (at 950 ps) a major conformational transition occurs within the modified pair

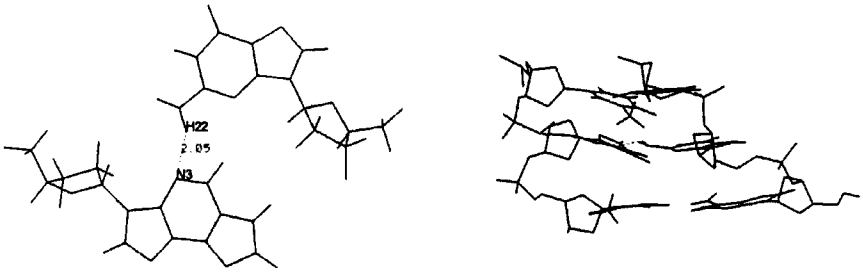

FIG. 6. Simulation #1. Snapshot showing the pair α-εdA / dG in the DNA duplex, representative for the last 250 ps of the simulation.

and the εA base is "hinged" in the direction of the major groove. As a result, the guanine is again exposed to the interior of the duplex where it can re-establish its stacking interactions and make hydrogen bonding contact with the εA base in opposition (cf. Fig. 7, conformation at the bottom). This is contrary to the situation in trajectory #1 and the first 950 ps of trajectory #2. This is an important example of the dynamical behaviour of the α-εdA / dG pair which is supported by means of molecular dynamics simulation. It was decided to extend this simulation for a further 100 ps in order to test the stability of the conformation adopted in the final stage of the 1 ns run. As expected, the two hydrogen bonds formed in the modified pair: [guanine]N(1)-H···N(6)[εA] and [guanine]N(2)-H···N(7)[εA] (Fig. 7) increased the stability of the duplex and the helical parameters (cf. Table 5) also adopted values closer to those of the unmodified duplex. This could suggest that the model has achieved a stable conformation.

CONCLUSION

DNA duplexes containing the fluorescent α-anomeric 1,N(6)etheno-deoxyadenosine residue placed between two neighbouring thymidines and in opposition to all four canonical nucleobases exhibit considerable thermodynamical stability. The duplex with the α-εdA / dG base opposition is most stable while the α-εdA / dC structure is the least stable. Fluorescence anisotropy measurements show that all structures with the exception of the α-εdA / dG case exhibit significant conformational flexibility. In the case of the duplex containing the α-εdA / dG base pair the rotational freedom of α-εdA is strongly blocked since the fast anisotropy component is not observed. This correlates with the results of molecular dynamics simulations for the α-εdA / dG duplex which shows a conformational drift from the unstacked, externally oriented fluorophore *via* an intermediate state, with the εA base weakly hydrogen bonded to guanine, to the formation of the strongly bonded α-εdA / dG pair. In the course of this conformational change, a transient formation of a severely kinked DNA duplex form was observed.

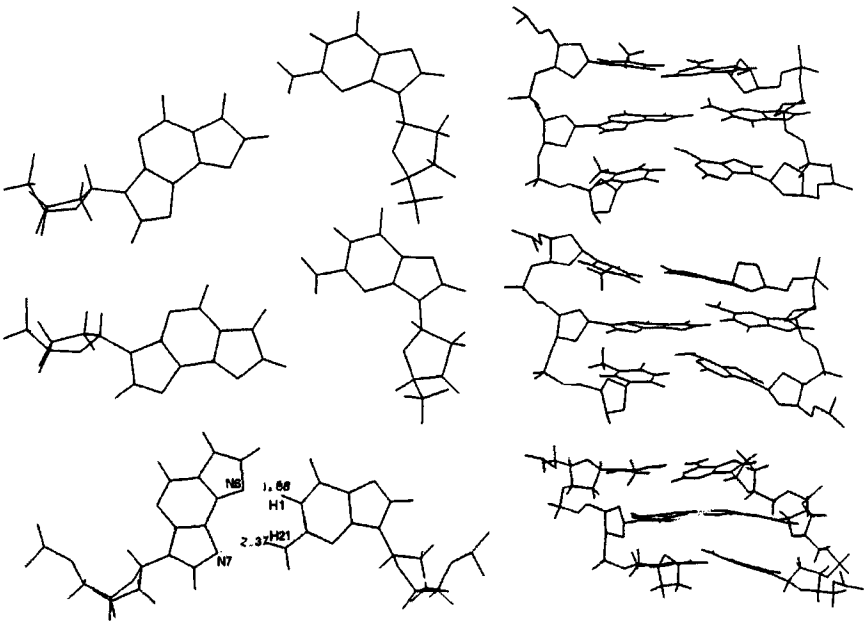

FIG. 7. Simulation #2. Conformational drift for the nucleoside pair α-εdA / dG of the duplex. Two top snapshots taken from the period before 950 ps. The bottom snapshot is representative for the last 50 ps.

The results presented herein clearly show that the β to α anomerisation of the nucleosidic fluorophore is not able to withstand the base stacking and pairing structural forces promoting regular DNA duplex formation. To further elucidate this observation, obtaining structural details on other duplexes, especially the one containing the α-εdA / dC base opposition, should be informative.

EXPERIMENTAL

General.

All chemicals used were obtained from Sigma-Aldrich. UV absorption was measured on a Perkin-Elmer Lambda-17 spectrophotometer. Fluorescence spectra were collected on a Perkin-Elmer MPF 66 spectrofluorometer. Short column chromatography was performed on silica gel 60H and RP-silica gel (Merck). High-performance liquid chromatography (HPLC) of oligomers was carried out with a Waters 600E instrument, using a multisolvent delivery system, equipped with 991 photodiode array and 470 fluorescence detectors. Reversed-phase columns, NovaPak C18 and DeltaPak C-4 (Waters) were used with isocratic and gradient modes (acetonitrile in 0.1 M aq. ammonium acetate). High resolution liquid secondary ion mass spectral analysis (HR-LSIMS) was performed on AMD Intecra Model 604 double focusing, reversed

geometry instrument fitted with cesium ion gun operating at ion energy of about 12 keV and accelerating voltage 8 kV.

Synthesis of α-1,N(6)etheno-deoxyadenosine.

α-Deoxyadenosine (1g, 4mmol) was dissolved in water (100ml) and treated dropwise with 1.5M aq. solution of chloracetaldehyde (20ml, 30 mmol) under pH-controlled conditions (addition of 1M KOH to get pH 3.5-4.5) at room temperature. Both steps of reaction were monitored by TLC (butanol/water/acetic acid 5: 3: 2 v/v, R_F=0.32 intermediate, 0.43 fluorescent product). After 3 days the reaction mixture was concentrated in a high vacuum. During this process saturated $NaHCO_3$ was added dropwise to suppress acid promoted depurination of the product. Oily residue was treated with ethanol, salts were filtered and concentrated filtrate subjected to fractionation on silicagel column chromatography using ethanol gradient in chloroform. Pure α-1,N(6)etheno-deoxyadenosine was obtained (0.67g, 60% yield) as amorphous powder. UV((H_2O): λ_{max} (nm)(ε): 266(6000); fluorescence (H_2O): λ_{max}^{Em} 420 nm; ^1H NMR (DMSO-d_6): δ (ppm), 9.29 (s, 1, 2H), 8.54 (s, 1, 8H), 8.07 (d, 1, 11H), 7.55 (d, 1, 10H), 6.48 (dd, 1, 1'H), 5.48 (d, 1, 3'OH), 4.85 (t, 1, 5'OH), 4.35 (m, 1, 3'H), 4.19 (m, 1, 4'H), 3.51 (m, 2, 5'5"H), 2.73-2.28 (m, 2, 2'2"H). HR-LSIMS: calculated for $[M+H]^+$ $C_{12}H_{14}N_5O_3$ = 276.10965, found = 276.10956.

UV Melting Measurements and the Protocol for Evaluation of Thermodynamic Parameters.

The optical melting profiles were measured on a Beckman DU70 spectrophotometer equipped with a multicell holder and a temperature control unit interfaced with PC. Oligomers were dissolved in 15mM phosphate buffer pH 7.0 with 1M NaCl. Their concentrations were determined spectrophotometrically using the Borer's method. For the 1,N(6)-ethenoadenine chromophore a value of 6000 L M^{-1} cm^{-1} for ε was taken. To ensure a correct duplex formation, equimolar amounts of appropriate single strands were mixed and heated in a cuvette to 80°C for 5 min and then gently cooled to 5°C within 2 h. Concentrations of duplexes ranging from 10^{-3} M to 10^{-5} M, as calculated for single strands, were used. The absorbance at 260 nm was measured as a function of temperature for five samples simultaneously. The temperature was changed at a rate of 0.5°C/min. To evaluate thermodynamic parameters the melting curves were fitted to a two-state model with sloping baselines using a nonlinear least-squares program kindly provided by Prof. Douglas H. Turner. Typical error estimate for the ΔH^o and ΔS^o values is ±13 %.

Steady-State and Time-Resolved Fluorescence Measurements.

All duplexes used for fluorescence studies were formed by titration of the α-εdA-labelled strand with each of the four complementary strands. Titration experiments were performed by placing a 400μL aliquot of a phosphate buffer solution containing the labelled strand into a fluorescence cuvette followed by addition of 10μL aliquots of the stock solution of the complementary strand. The hybridisation process was followed by absorption and emission spectra as a function of molar equivalent of complementary strand added. Both absorption and emission spectra were corrected for the changes in the volume of the titrated solution. Fluorescence spectra were measured

on a Perkin Elmer LS50 B spectrofluorometer equipped with thermostated cell holders. Fluorescence lifetimes and anisotropic decays were determined by time-correlated single-photon counting on a picosecond laser system described[27]. The overall instrument response time was 32 ps FWHM. The samples were excited at 310 nm with vertically polarised laser pulse and emission collected at 400 nm. For the lifetime measurements two sets of data (512 channels) were collected: the instrument response profile (laser pulse) and fluorescence with the emission polariser (Glan-Thompson) set at the "magic angle" (54.7°)[23] with respect to the vertical excitation to eliminate rotational diffusion artefacts. In case of anisotropic decays two additional data sets (1024 channels) for crossed and parallel orientations of emission and excitation polarisers were collected in 1 min cycles. The cycle was repeated until a sufficient number of counts (at least 70000) in the parallel decay data file was collected. The experimental decay curves were analysed using an IBH Consultants Ltd. (Glasgow) decay analysis software Version 4.

Model building and molecular dynamics simulation

The initial structures were built as canonical B-DNA duplexes using the procedures provided in the AMBER 4.1 package[28]. The α-εdA residue was defined according to the AMBER 4.1 model definition standards. The model molecules were added 20 sodium counterions (3.5 Å from the phosphate centers) and solvated in a rectangular PBC box with 10 Å thick water layer in all dimensions around the molecule (Edit module applied). Simulations were carried out using the Sander program (part of the AMBER 4.1 package) run on a CRAY J-916 machine in the Poznañ Supercomputing and Networking Center. The force field parameters and atomic partial charges of the modified nucleoside were developed using the Gaussian 94[29] and Resp[30] programs. We have also confirmed that the α-anomerization does not affect the distribution of charges in the nucleoside. The protocol for the simulations followed the procedure applied by T. E. Cheatham and P. A. Kollman[31] and consisted of an equilibration procedure (alternating energy minimization and short molecular dynamics runs with gradually relieved constraints on the DNA molecule) and 1 ns of molecular dynamics in 300 K with the long-range electrostatic interactions treated using the particle-mesh Ewald summation method. The SHAKE algorithm for maintainig the X-H atomic distances was used and the time-step for the Newtonian equations integration was set to 2 fs. The resultant trajectories from all simulations were analysed and visualised on an Iris Indigo^2 workstation using the InsightII software (MSI), the CURVES 5.1 program[25] and our own procedures.

Acknowledgements. This work was supported by grants from the State Committee for Scientific Research, Republic of Poland (3T09A11412) to R. W. A. and the Natural Sciences and Engineering Research Council of Canada (NSERC) to R. E. V. The authors thank Prof. Douglas H. Turner for providing software for evaluation of thermodynamic parameters and Grazyna Dominiak for technical assistance. Access to the resources of the Poznañ Supercomputer and Networking Center is acknowledged.

REFERENCES

1. de los Santos, C.; Kouchakdjian, M.; Yarema, K.; Basu, A.; Essigmann, J.; Patel, D. J. *Biochemistry*, **1991** ***30***, 1828-1835.

2. Leonard, G. A.; McAuley-Hecht, K. E.; Gibson, N. J.; Brown, T.; Watson, W. P.; Hunter, W. N. *Biochemistry*, **1994** ***33***, 4755-4761.
3. Skalski, B.; Bartoszewicz, J.; Paszyc, S.; Gdaniec Z.; Adamiak, R.W. *Tetrahedron*, **1987** ***43***, 3955-3961.
4. Skalski, B.; Paszyc, S.; Adamiak, R.W.; Steer, R.P.; Verrall, R.E. *J. Chem. Soc. Perkin Trans. II*, **1989**, 1691-1696
5. Burdzy, A.; Skalski, B.; Paszyc, S.; Adamiak, R. W.; Popenda, M.; Adamiak, R. W. *Acta Biochim. Pol.*, **1998** ***45***, 941-948.
6. Ide, H.; Shimizu, H.; Kimura, Y.; Sakamoto, S.; Makino, K.; Glackin, M.; Wallace, S. S.; Nakamuta, H.; Sasaki, M.; Sugimoto, N. *Biochemistry*, **1995** ***34***, 6947-6955.
7. Tyoufumi,Y.; Mineo, S. *Chem.Pharm.Bull.*, **1984** ***32***, 1441-1450.
8. Biernat, J.; Ciesiolka, J.; Gornicki, P.; Adamiak, R.W.; Krzyzosiak, W.; Wiewiorowski, M. *Nucleic Acids Res.*, **1978** ***5***, 784-804.
9. Borer, P. N.; Dengler, B.; Tinoco Jr. I.; Uhlenbeck, O. C. *J. Mol. Biol.*, **1974** ***86***, 843-853
10. Freier, S. M.; Burger, B. J.; Alkema, D.; Neilson, T.; Turner, D. H. *Biochemistry*, **1983** ***22***, 6198-6206
11. Petersheim, M.; Turner, D. H. *Biochemistry*, **1983** ***22***, 256-263.
12. Gralla, J.; Crothers, D.M. *J.Mol.Biol.*, **1973** ***78***, 301-319.
13. Breslauer, K. J.; Frank, R.; Blocker, L. A.; Marky, A. *Proc. Natl. Acad. Sci. USA*, **1986** ***83***, 3746-3751.
14. Peyret, N.; Senevirante, P. A.; Allawi, H. T.; SantaLucia, J. Jr. *Biochemistry*, **1999** ***38***, 3468-3477.
15. Tolman, G. L.; Bario, J. R.; Leonard, N. J. *Biochemistry*, **1974** ***13***, 4869-4878.
16. Steiner, R. F.; Kinnier, W.; Lunasin, A.; and Delac, J. *Biochem. Biophys. Acta*, **1973** ***294***, 24-28.
17. Janik, B.; Sommer, R. G.; Kotick, M. P.; Wilson, D. P.; and Erickson, R. J. *Physiol. Chem. Phys.*, **1973** ***5***, 27-36.
18. Lakowicz, J.R. *Principles of Fluorescence Spectroscopy*, **1986** Plenum Press; New York
19. Penzer, G. R. *Eur. J. Biochem.*, **1973**, ***34***, 297-305.
20. Ferreira, S. T.; Gratton, E. *J. Am. Chem. Soc.*, **1994**, ***116***, 5791-5795.
21. Collini, M.; Chirico, G.; Baldini, G.; Bianchi, M. E. *Biopolymers*, **1995**, ***36***, 211-225.
22. Cornell, W. D.; Cieplak, P.; Bayly, C. I.; Gould, I. R.; Merz, Jr. K. M.; Ferguson, D. M.; Spellmeyer, D. C.; Fox, T.; Caldwell, J. W.; Kollman, P. A. *J. Am. Chem. Soc.*, **1995** ***117***, 5179-5197.
23. Essmann, U.; Perera, L.; Berkowitz, M. L.; Darden, T.; Lee, H.; Pedersen, L. G. *J. Chem. Phys.*, **1995** ***103***, 8577-8593.
24. Auffinger, P.; Westhof, E. *Curr. Opin. Struct. Biol.*, **1998** ***8***, 227-236.
25. Lavery, R.; Sklenar, H. *J. Biomol. Str. Dyn.*, **1988** ***6***, 63-91.

26. Dickerson, R. E. *Nucleic Acids Res.*, **1998** ***26***, 1906-1926.
27. Augustyniak, W.; Koput, J.; Maciejewski, A.; Sikorski, M.; Steer, R. P.; Szymanski, M. *Polish J. Chem.*, **1993** ***67***, 1409-1423.
28. Pearlman, D. A.; Case, D. A.; Caldwell, J. W.; Ross, W. S.; Cheatham, T. E.; Ferguson, D. M.; Seibel, G. L.; Singh, U. C.; Weiner, P.; Kollman, P. A. *AMBER Version 4.1*. **1995** University of California.
29. *Gaussian 94, Revision C.3.* Gaussian Inc., Pittsburgh 1995.
30. Bayly, C. I.; Cieplak, P.; Cornell, W. D.; Kollman, P. A. *J. Phys. Chem.*, **1993** ***97***, 10269-10280.
31. Cheatham, T. E.; Kollman, P. A. *J. Am. Chem. Soc.*, **1997** ***119***, 4805-4825.